Anisotropic transferred hyperfine interactions in Cs_2CuCl_4

2008 J. Phys.: Condens. Matter 20 295225

(http://iopscience.iop.org/0953-8984/20/29/295225)

J. Phys.: Condens. Matter **20** (2008) 295225 (8pp) doi:10.1088/0953-8984/20/29/295225

Anisotropic transferred hyperfine interactions in Cs_2CuCl_4

M-A Vachon[1], G Koutroulakis[1], V F Mitrović[1], A P Reyes[2], P Kuhns[2], R Coldea[3] and Z Tylczynski[4]

[1] Department of Physics, Brown University, Providence, RI 02912, USA
[2] National High Magnetic Field Laboratory, Tallahassee, FL 32310, USA
[3] Department of Physics, University of Bristol, Bristol BS8 1TL, UK
[4] Institute of Physics, Adam Mickiewicz University, Umultowska 85, 61-614 Poznan, Poland

E-mail: vemi@brown.edu (V F Mitrović)

Received 24 January 2008, in final form 9 May 2008
Published 1 July 2008
Online at stacks.iop.org/JPhysCM/20/295225

Abstract

We report ^{133}Cs nuclear magnetic resonance (NMR) measurements of magnetic insulator Cs_2CuCl_4 in the paramagnetic phase ($T \geqslant 4.2$ K) as a function of the orientation of an applied magnetic field with respect to the principal crystalline axes. The magnetic shift tensor is determined. It is found that its principal axes do not coincide with the principal axes of the crystal. The Cu–Cs dipolar interaction tensor is calculated as well. From these, we deduce the full transferred hyperfine tensor for the two inequivalent Cs sites of the unit cell. We find that the tensors are anisotropic, containing non-zero off-diagonal terms, and that the transferred hyperfine coupling between Cu electronic spins and Cs nuclei dominates the NMR shift on both Cs sites.

(Some figures in this article are in colour only in the electronic version)

1. Introduction

Many fascinating phenomena can arise in spin-1/2 antiferromagnets (AFs) as a result of an interplay between the geometric frustration and quantum fluctuations. One such example is atypical spin dynamics in the 2D spin-1/2 anisotropic triangular AF Cs_2CuCl_4 as revealed by neutron scattering [1, 2]. Furthermore, at low temperatures many exotic phases are induced in that compound in the presence of a magnetic field [3, 4]. As a local probe, NMR is well suited to study microscopic spin structure and low energy spin dynamics in these phases. This is because nuclear spins couple to electronic spins and are sensitive to the local electronic spin arrangement. However, to be able to infer the microscopic electronic spin structure, knowledge of the hyperfine coupling between nuclei and electronic spins is required. The entire hyperfine tensor can be obtained through detailed measurements of NMR spectra as a function of the magnetic field orientation. Such a study is described in this manuscript and the full hyperfine tensor is deduced. The aim of this work is to acquire a detailed understanding of the effect of magnetism on Cs NMR.

In our previous work [5] we showed that the ^{133}Cs NMR shift in Cs_2CuCl_4 is dominated by the Cu spin degrees of freedom through a strong anisotropic hyperfine coupling. However, only the magnitude of the coupling along the principal crystal axes was determined. The paper of Hartmann *et al* [6] describes a room temperature NMR study of the isostructural compounds Cs_2MX_4 (M = Cu, Co, Zn and X = Cl, Br), where the tensors of the nuclear quadrupole coupling and the magnetic shift were determined. Here, we present the determination of the full transferred hyperfine tensor for the two inequivalent Cs sites in the paramagnetic phase ($T \geqslant 4.2$ K) of Cs_2CuCl_4. The transferred hyperfine tensor on both Cs sites is found to be anisotropic. The tensor was deduced from the ^{133}Cs NMR spectra of single crystal Cs_2CuCl_4 recorded as a function of the orientation of the applied magnetic field ($H_0 = 5$ T) with respect to the principal crystal axes at three different temperatures, $T = 293$, 81, and 4.2 K. Furthermore, the magnitude of the diagonal terms was determined from measurements in the fully polarized state at $H_0 > 9$ T and $T < 1$ K.

The paper is organized as follows. We describe the experimental details in section 2.1. In section 2.2 we discuss basic principles and assumptions necessary for the analysis of the data. In section 3.1 the temperature dependence of the quadrupole coupling parameters is discussed. Measurements

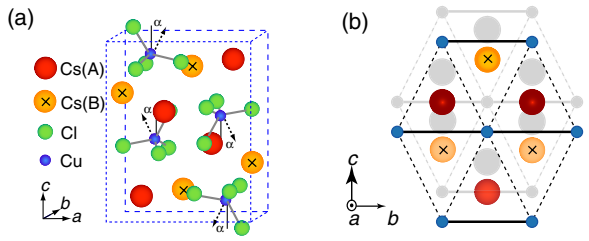

Figure 1. (a) The orthorhombic unit cell of Cs_2CuCl_4 with the four independent Cu spins (Cu^{2+} ions) displayed as the smallest spheres in the center of the tetrahedra formed by the Cl^- ions (bigger, green spheres). The dashed lines and arrows indicate the local symmetry axis at each Cu site [10]. The arrows pointing above the (bc)-plane denote the even Cu chains while the ones pointing below the plane denote the odd chains. Two inequivalent Cs sites Cs(A) and Cs(B) are depicted as denoted. Lattice parameters are $a = 9.65$ Å, $b = 7.48$ Å, and $c = 12.35$ Å [8]. (b) Triangular magnetic lattice with exchange couplings of $J = 0.375$ meV along solid lines and $J' = 0.125$ meV along dashed lines. Darker Cs atoms are located slightly above the spin (bc) plane and lighter ones below the plane. The neighboring planes are offset by $0.34c$.

of the spin shift for the different orientations of the magnetic field and deduction of the magnetic shift tensor are presented in section 3.2. We calculate the dipolar fields in section 3.3 and the full transferred hyperfine tensor is obtained in section 3.4.

2. Experiment

2.1. Sample and experimental technique

Large single crystals of Cs_2CuCl_4 grown from an aqueous solution were used in this study [7]. Their orthorhombic crystal structure with *Pnma* [8] space group is shown in figure 1(a). Each copper atom is surrounded by four chlorine ones that form a distorted tetrahedron. The axis of symmetry of these tetrahedra is represented by arrows in figure 1(a). Their orientation is staggered by an angle $\pm\alpha \simeq 35°$ along the c-axis direction and rotated by 180° between planes [9]. The magnetic lattice is formed by a linear chain of the tetrahedra in the b-direction with two Cl between each Cu and by stacking of the chains along the c-direction, displaced by $b/2 = 3.74$ Å with respect to each other. Two types of chains can be discerned. The chains where the axis of symmetry of the tetrahedra (arrows in figure 1(a)) points above and below the (bc)-plane are referred to as even and odd, respectively. The planes are stacked together along the a-axis and displaced with respect to each other as depicted in figure 1(b). The material is an insulator with each magnetic Cu^{2+} ion carrying spin $S = 1/2$, forming a frustrated triangular lattice in the (bc)-plane [10]. The superexchange routes are mediated by two nonmagnetic Cl^- ions. The two inequivalent Cs sites, labeled as Cs(A) and Cs(B), in the unit cell are shown in figure 1 as well. The Cs(A) site is located in the center of the triangle formed by the Cu spins, while Cs(B) is closer to the base of the triangle and further away from the spin plane than Cs(A).

The volume of a typical sample used in our experiment was of the order of 10 mm^3. The crystallographic axes were determined by x-ray Laue diffraction. The faces were cut perpendicular to the crystal axes. The sample was mounted to one of the crystal faces and rotated with respect to the applied field about an axis using a single axis goniometer. The rotation angle was inferred from the signal of two perpendicularly positioned Hall sensors.

The measurements were done using a high homogeneity NMR magnet in an applied field of 5 T. The temperature control was provided by a continuous flow cryostat. The NMR data were recorded using a state-of-the-art homemade NMR spectrometer. NMR spectra were obtained from the sum of spin-echo Fourier transforms recorded at each 100 KHz intervals. Since the ^{133}Cs nuclear spin is $I = 7/2$ and both Cs sites are in non-cubic environments, seven distinct quadrupolar satellite lines are observed. The shift was obtained from the position of the central peak using a gyromagnetic ratio of $\gamma = 5.5844$ MHz T^{-1}.

2.2. Theoretical background

The NMR shift K is generally defined such that the observed NMR frequency obeys the equation

$$\omega \equiv \gamma H_0(1 + K), \tag{1}$$

where γ is the gyromagnetic ratio of the nuclear spin, H_0 the applied magnetic field, and $K \equiv H_{\rm loc}/H_0$ is the shift. Thus, K is a measure of the relative strength of the component of the local magnetic field ($H_{\rm loc}$) parallel to the applied magnetic field, H_0. In the more general case where the shift varies as a function of the orientation of H_0 (anisotropic shift), the scalar K is promoted to a second-rank tensor $\mathbb{K}$ and the expression for the observed NMR frequency becomes [11, 12]

$$\omega = \gamma H_0(1 + \hat{\mathbf{h}} \cdot \mathbb{K} \cdot \hat{\mathbf{h}}), \tag{2}$$

where $\hat{\mathbf{h}} = \mathbf{H}_0/H_0$ is a unit vector in the direction of the applied magnetic field.

For Cs nuclei in Cs_2CuCl_4 the main source of the local field is the $S = 1/2$ Cu electronic spins. From an NMR point of view, it is important to have a good understanding of the electron–nucleus interaction in order to retrieve relevant physical information such as microscopic electronic spin configuration. The Hamiltonian describing the interaction between a nuclear spin $\mathbf{I}$ and electronic spins $\mathbf{S}_N$ is in general written as [12, 13]

$$\mathcal{H} = -\gamma\hbar\mathbf{I} \cdot \sum_N \mathbb{M}_N \cdot (\mathbf{g}\mu_{\rm B}\mathbf{S}_N)\,. \tag{3}$$

Here, $\mathbb{M}_N$ is a second-rank tensor specifying the coupling between the nuclear spin and the different electronic spins, $\mathbf{S}_N$, and $\mathbf{g}$ is the electronic g-factor with the following components along the principal crystal axes: $g_a = 2.27$, $g_b = 2.11$, and $g_c = 2.36$ [3]. In solids such as Cs_2CuCl_4 with small quadrupolar interaction, the most common contributions to the tensor $\mathbb{M}_N$ are the dipolar interaction tensor $\mathbb{D}_N$ and the transferred hyperfine interaction tensor $\mathbb{A}_N$. Therefore, $\mathbb{M}_N$ can be expressed as

$$\mathbb{M}_N = \mathbb{D}_N + \mathbb{A}_N, \tag{4}$$

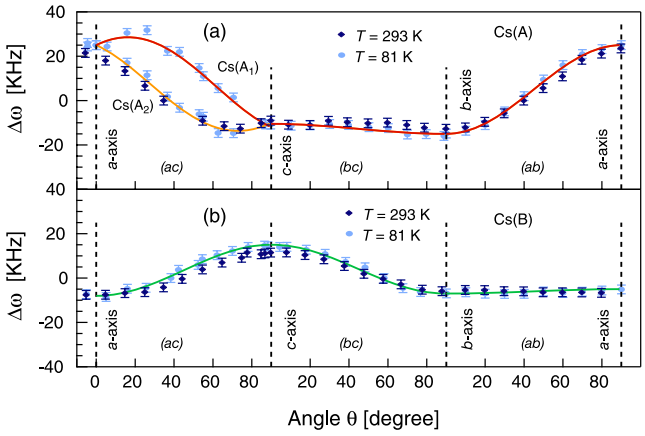

Figure 2. The separation between two adjacent quadrupolar-split satellites as a function of the orientation of the applied field at 5 T with respect to the crystal axes at $T = 293$ and 81 K for Cs(A), upper panel, and Cs(B), lower panel. At $T = 81$ K two inequivalent sites, labeled $Cs(A_1)$ and $Cs(A_2)$, are observed for certain orientations of the field. Solid lines are fits of the $T = 81$ K data to expressions in equation (13).

with the components of the dipolar tensor given by

$$\left(D_{ij}\right)_N = \frac{\mu_0}{4\pi}\left[\frac{\delta_{ij}}{r_N^3} - \frac{3(r_i)_N(r_j)_N}{r_N^5}\right], \tag{5}$$

where μ_0 is the permeability of the vacuum and r_N the distance between the nuclear spin and the electronic spin $\mathbf{S}_N$.

Using the definition of the Zeeman energy $\mathcal{H}_0 = -\boldsymbol{\mu}\cdot\mathbf{H}_0$ and $\boldsymbol{\mu} = \gamma\hbar\mathbf{I}$, it follows from equations (3) and (4) that

$$\mathbf{H}_{\rm loc} = \mathbf{g}\mu_{\rm B}\left(\mathbb{D}_N + \mathbb{A}_N\right)\cdot\mathbf{S}_N \qquad \text{and} \qquad K = \frac{\mathbf{H}_{\rm loc}\cdot\hat{\mathbf{h}}}{H_0}. \tag{6}$$

Evidently, if the principal axes of the tensor coincide with the principal axes of the crystal, the tensor $\mathbb{M}_N$ will be diagonal. However, in most complex materials, the principal axes do not coincide and the tensor $\mathbb{M}_N$ is not diagonal when expressed in the crystallographic coordinate system (O_{abc}). In that case, it is useful to find the particular coordinate system O_{xyz} in which the tensor will be diagonal and a rotation matrix $\mathbb{R}$ that transforms quantities from one coordinate system into the other ($\tilde{\mathbb{A}} = \mathbb{R}^{\rm T}\cdot\mathbb{A}\cdot\mathbb{R}$). In the O_{xyz} coordinate system, all of the off-diagonal terms of the shift tensor $\mathbb{K}$ vanish and equation (2) becomes

$$\omega = \gamma H_0\left[1 + \sum_\alpha K_\alpha \hat{h}_\alpha^2\right], \tag{7}$$

where the summation is over the principal axes of the shift tensor, i.e. $\alpha = \{x, y, z\}$.

The matrix $\mathbb{R}$ depends on the detailed electronic configuration in the material and is therefore very difficult to estimate. However, its form can be determined experimentally by recording the NMR spectra as a function of the orientation of the applied magnetic field with respect to the crystal axes.

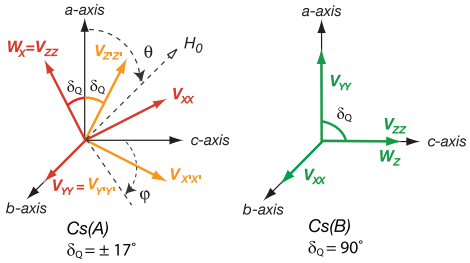

Figure 3. Coordinate systems showing the principal crystallographic axes O_{abc}, the principal axes O_{xyz} of the quadrupolar splitting tensor, and the principal axes of the quadrupolar tensor O_{XYZ} for Cs(A) and Cs(B). θ and φ define the angle between the direction of the applied field and the principal crystal axes.

3. Results and discussion

We will first discuss quadrupolar parameter measurements to be able to understand detailed spectral features. Then, we will proceed to the analysis of the spectra as a function of the magnetic field orientation.

3.1. Quadrupole splitting

When the quadrupole interaction is taken into account, equation (1) becomes [11, 12],

$$\omega = \gamma(1+K)H_0 + \omega_Q(m-1/2) \times \left(3\cos^2\theta_Q - 1 + \eta\sin^2\theta_Q\cos 2\varphi_Q\right) \tag{8}$$

up to second order in perturbation theory. The second term accounts for the quadrupole interaction for each $m \leftrightarrow m \pm 1$ transition. Here, θ_Q and φ_Q are the angles between the applied field and the principal axes of the electric field gradient (EFG), shown in figure 3 and defined so that $|V_{ZZ}| \geqslant |V_{XX}| \geqslant |V_{YY}|$ and eq $\equiv V_{ZZ}$. The asymmetry parameter η is defined as $\eta \equiv (V_{XX} - V_{YY})/V_{ZZ}$. The quadrupolar frequency equals $\omega_Q = 3e^2qQ/(\hbar 2I(2I-1))$, where Q and q are the nuclear and electronic quadrupole moments.

In figure 2 the average separation between two adjacent quadrupolar satellite transitions, $\Delta\omega$, is plotted as a function of the angle between the principal crystal axes and the applied field at $T = 81$ and 293 K for Cs(A) and Cs(B). Within the error bars, no significant difference in $\Delta\omega$ values is observed as temperature is lowered from $T = 293$ to 81 K. The separation values can be used to deduce the quadrupolar parameters. If the principal axes of the EFG tensor were to coincide with those of the crystal, we could in principle have used equation (8) to deduce the quadrupole parameters. Since this is not the case in Cs_2CuCl_4, we introduce the quadrupolar splitting tensor $\mathbb{W}$ such that $\Delta\omega = \sum_\alpha W_\alpha\hat{h}_\alpha^2$ in the coordinate system O_{xyz} where $\mathbb{W}$ is diagonal. Here, $\alpha = \{x, y, z\}$ and $\hat{\mathbf{h}}$ is the unit vector along the applied field.

We then use $\tilde{\mathbb{W}} = \mathbb{R}^{\rm T}\cdot\mathbb{W}\cdot\mathbb{R}$ to express $\Delta\omega$ in the coordinate system of the crystal. The results have the same dependence on angles as in the set of equations (13) for the shift, as discussed in section 3.2. The correspondence between the principal axes of the EFG tensor and those from the quadrupolar splitting tensor is such that V_{ZZ} will point along

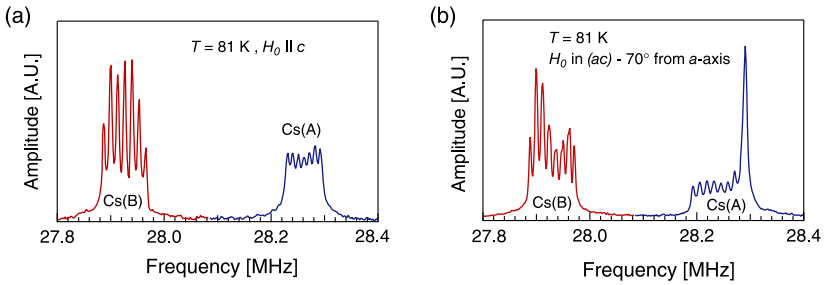

Figure 4. ^{133}Cs NMR spectra at $T = 81$ K and at 5 T applied magnetic field. (a) Spectrum for field applied along the c-axis. The spectrum is characterized by two sets of lines corresponding to the two inequivalent sites Cs(B) and Cs(A). (b) Spectrum for field applied in the (ac)-plane at an angle of 70° from the a-axis. Additional resonance peaks, beyond seven quadrupolar satellites, reveal the presence of another inequivalent site.

Table 1. Quadrupole frequency ω_Q, the asymmetry parameter η, angle δ_Q, and the direction of the principal axes of the EFG tensor at $T = 293$ and 81 K. Results from [6] at $T = 293$ K are also reported for comparison.

T (K)			ω_Q (KHz)	η	δ_Q (deg) (from a-axis)
293	Cs(A)	This work	11.5 ± 1.0	0.06 ± 0.04	17 ± 1
		Ref. [6]	11.75	0.038	16.1
293	Cs(B)	This work	6.0 ± 1.0	0.16 ± 0.04	90 ± 2
		Ref. [6]	6	0.176	93.2
81	Cs(A)	This work	14.5 ± 2.0	0.05 ± 0.03	17 ± 1
81	Cs(B)	This work	7.3 ± 1.0	0.17 ± 0.03	90 ± 2

$\max(\{W_\alpha\})$, different for both Cs(A) and Cs(B), as shown in figure 3. Combining these results with equation (8), we find that the relevant quadrupole parameters, ω_Q and η [14], are given by

$$\begin{aligned} &W_x = 2\omega_Q, && W_y = \omega(1-\eta), \\ &&& W_z = \omega(1+\eta), && \text{for Cs(A)}, \\ &W_x = \omega(1+\eta), && W_y = \omega(1-\eta), \\ &&& W_z = 2\omega_Q, && \text{for Cs(B)}. \end{aligned} \tag{9}$$

Their values are summarized in table 1 as well as the orientation of the principal axis of the EFG tensor. Our room temperature results are comparable with those in [6]. Furthermore, the parameters at $T = 81$ K are consistent with the splittings at $T = 2$ K deduced from the beats in the spin–spin relaxation profile [5]. Therefore, we infer that any significant change of the quadrupolar parameters, and consequently of the crystal structure of the material, occurs as temperature is lowered from room temperature down to $T = 80$ K. For Cs(A), V_{ZZ} points $\delta_Q \simeq \pm 17°$ away from the a-axis in the (ac)-plane, as sketched in figure 3. The direction of V_{ZZ} coincides with the c-axis for Cs(B).

3.2. Rotation studies

In figure 4(a) ^{133}Cs spectra at $T = 81$ K and $H_0 = 5$ T applied along the c-axis are shown. Two sets of lines correspond to crystallographically inequivalent Cs sites, Cs(A) and Cs(B), respectively. Seven quadrupolar satellites are evident for both sites. The satellites are separated by 14.1 kHz for Cs(A) and 14.7 kHz for the Cs(B) site. For Cs(A) we observe that the intensities of all satellite transitions are comparable to the intensity of the central transition. It is not clear what causes these peaks to have equal intensities.

When the applied field is rotated away from the c-axis in the (ac)-plane, each of these sites splits into two sites, as illustrated in figure 4(b). For example, in a magnetic field applied in the (ac)-plane 70° away from the a-axis, the Cs(A) spectrum consists of seven lower intensity peaks and one higher intensity peak. The intensity of the higher peak is approximately seven times larger than the intensity of one of the seven equidistant small peaks. This suggests the splitting of the magnetic unit cell that causes the partition of the Cs(A) into two crystallographically inequivalent sites, Cs(A $_1$) and Cs(A_2). The quadrupole splitting for Cs(A_1) is $\Delta\omega = 12.4$ kHz, while that for Cs(A_2) is negligible, i.e. $\Delta\omega <$ 2 kHz, as evident in both figures 4(b) and 2. For this particular orientation the central peak frequencies of Cs(A_1) and Cs(A_2) are separated by 60 kHz. This separation depends on the field orientation, as will be discussed in detail below. The splitting of the Cs(B) into two inequivalent sites, Cs(B_1) and Cs(B_2), is barely noticeable for this field orientation.

The dependence of the NMR spectra peak frequency on the orientation of the magnetic field at $T = 4.2$ K is plotted in figure 5. The magnetic field is rotated with respect to all three principal crystal axes. The peak frequency is traced since at $T = 4.2$ K quadrupolar satellites cannot be discerned due to magnetic line broadening [5]. The angular dependence of the peak frequency at $T = 81$ and 293 K exhibits a similar periodicity.

For the rotation of the field in the (ac)-plane, each Cs(A) and Cs(B) resonance line splits into two. No such splitting is

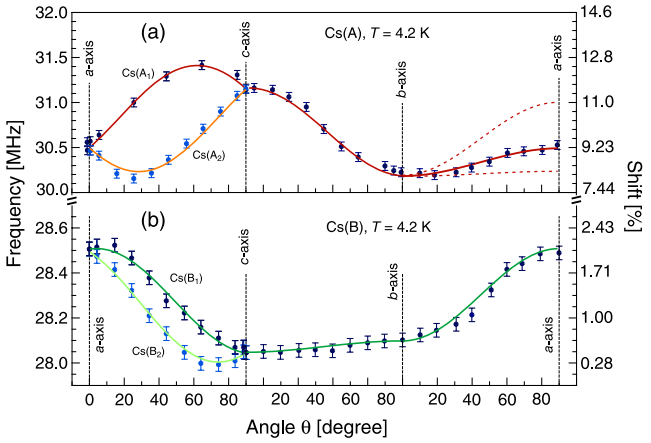

Figure 5. Frequency of the peak of the NMR spectra at $T = 4.2$ K as a function of the angle between the applied field ($H_0 = 5$ T) and one of the principal crystal axes for Cs(A) (a) and Cs(B) (b). The double resonance lines in the (ac)-plane are observed for each Cs(A) and Cs(B) sites. The solid lines are the result of a fit to equation (12). The dashed line denotes the peak frequency when the field was rotated about an axis 20° away from the c-axis in the (ab)-plane.

detected when the field is rotated in the (bc) and (ab)-planes. These observations indicate that the splitting of the Cs(A) and Cs(B) resonance into two lines occurs only when the magnetic field is misaligned with respect to the principal crystal axes in the (ac)-plane. Indeed, if the field is rotated exactly about the c-axis in the (ab)-plane no such splitting is observed. This splitting, apart from being orientation dependent, also depends on the temperature and strength of the applied magnetic field. In the paramagnetic state, the temperature dependence of the splitting is the same as that of the shift, described by a Curie–Weiss law having a Curie–Weiss temperature of ∼4 K [5]. This implies that the splitting is an NMR phenomenon reflecting an intrinsically anisotropic nature of the shift and the transferred hyperfine interaction. Since the splitting is absent when the field is exactly aligned along one of the principal crystallographic axes, we exclude the possibility that it is caused by the presence of staggered magnetization.

The data presented in figure 5 suffice to determine the full shift tensor $\mathbb{K}$. We outline how this can be achieved by identifying a form of the matrix $\mathbb{R}$, as described in section 2.2. A more general description of arbitrary rotations, i.e. a general form of the matrix $\mathbb{R}$, is described in [13]. However, considerations of the local symmetry of the crystal at the cesium site (point group C_s [9]) allow us to restrict the form of the matrix $\mathbb{R}$. The only allowed symmetry operation for this point group is a mirror symmetry $(a, b, c) \rightarrow (a, -b, c)$. An arbitrary tensor, $\mathbb{A}$, will transform under the mirror operation $\mathbb{M} = \mathrm{diag}(1, -1, 1)$ as:

$$\begin{pmatrix} A_{11} & A_{12} & A_{13} \\ A_{21} & A_{22} & A_{23} \\ A_{31} & A_{32} & A_{33} \end{pmatrix} \longrightarrow \begin{pmatrix} A_{11} & -A_{12} & A_{13} \\ -A_{21} & A_{22} & -A_{23} \\ A_{31} & -A_{32} & A_{33} \end{pmatrix}. \tag{10}$$

Since the tensor has to remain invariant under this transformation, A_{13} and A_{31} are the only off-diagonal terms that can have a non-zero value. Therefore, we may restrict our discussion to crystal coordinate systems O_{abc} that differ from O_{xyz}, defined by the shift tensor principal axes, only by a rotation of δ away from the a-axis in the (ac)-plane. In this new coordinate system O_{abc}, the tensor $\mathbb{K}$ takes the following form

$$\begin{aligned} \mathbb{K} &= \begin{pmatrix} K_x C^2 + K_z S^2 & 0 & (K_x - K_z)SC \\ 0 & K_y & 0 \\ (K_x - K_z)SC & 0 & K_z C^2 + K_x S^2 \end{pmatrix} \\ &\equiv \begin{pmatrix} K_a & 0 & K_{ac} \\ 0 & K_b & 0 \\ K_{ac} & 0 & K_c \end{pmatrix}, \end{aligned} \tag{11}$$

where $C \equiv \cos\delta$ and $S \equiv \sin\delta$. The contribution of $\mathbb{K}$ to the shift, as defined in equation (2), in an applied magnetic field, $\mathbf{H}_0 = (H_a, H_b, H_c) = H_0(\cos\theta, \sin\theta\sin\varphi, \sin\theta\cos\varphi)$, in the O_{abc} coordinate system is given by

$$\begin{aligned} K &= K_a \cos^2\theta + 2K_{ac}\cos\theta\sin\theta\sin\varphi \\ &\quad + K_b \sin^2\theta\cos^2\varphi + K_c \sin^2\theta\sin^2\varphi. \end{aligned} \tag{12}$$

Here, θ and φ are the angles between the direction of the applied field and the principal crystal axes, defined as shown in figure 6(a). In the coordinate system O_{xyz} the shift can be expressed as,

$$\begin{aligned} K &= K_x \cos^2(\theta - \delta) + K_z \sin^2(\theta - \delta) \\ &\qquad (ac)\text{-plane}, \\ K &= (K_x \sin^2\delta + K_z \cos^2\delta)\sin^2\varphi + K_y \cos^2\varphi \\ &\qquad (bc)\text{-plane}, \\ K &= (K_x \cos^2\delta + K_z \sin^2\delta)\cos^2\theta + K_y \sin^2\theta \\ &\qquad (ab)\text{-plane}. \end{aligned} \tag{13}$$

The consequences of the chosen local symmetry, C_s, of the tensor $\mathbb{K}$ are made clear by these expressions. Indeed, under the reflection of δ to $-\delta$, the expressions for the shift measured for the field applied in the (ab)-and (bc)-planes remain invariant. However, for the field applied in the (ac)-plane two distinct shifts are obtained. It should be noted that the maximum shift is obtained for $\theta = \delta$. This particular signature can be easily discerned experimentally allowing one to accurately determine the angle δ and the matrix $\mathbb{R}$.

The results of the fit to equation (12) for Cs(A) and Cs(B) sites are presented by the solid lines in figure 5. Setting the symmetry arguments aside, it is evident from the data that the form of the shift tensor in equation (11) is the appropriate one. In other words, in order to account for the observed splitting when the field is aligned away from the principal crystal axes in the (ac)-plane, it is necessary to set $K_{ac} = K_{ca} \neq 0$ and to allow the sign to change from one site to the other. Because no splitting is found when the field is rotated in the (bc)- and (ab)-planes, we set all other off-diagonal terms to zero. Thus, the form of the shift tensor found experimentally is in agreement with the local symmetry of the crystal at the Cesium site. Moreover, symmetry arguments confirm that off-diagonal terms K_{bc}, K_{cb}, K_{ab}, and K_{ba} are truly zero and not just arbitrarily small due to a limited experimental sensitivity.

The results of the fit at three different temperatures are summarized in table 2. The shift tensor for the Cs(A) site is

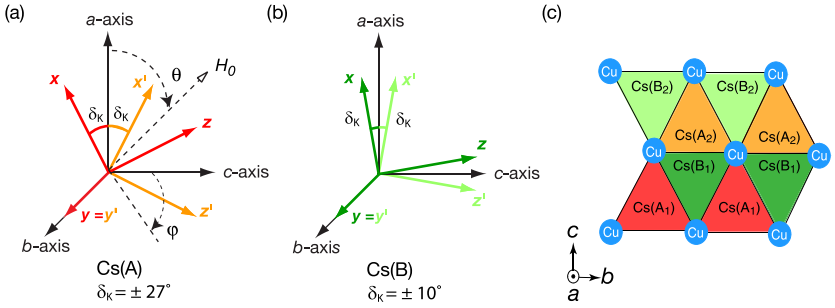

Figure 6. (a) and (b) Coordinate systems showing the principal crystallographic axes O_{abc} and the principal axes of the shift tensor, denoted by x, y, z. The x and x'-axes are rotated about the b-axis away from the a-axis by an angle $\delta_K = \pm 27°$ for Cs(A) and $\delta_K = \pm 10°$ for Cs(B). Angles θ and φ define the angle between the direction of the applied field and the principal crystal axes. (c) Schematic representation of the triangular lattice of Cu spins $S = 1/2$ (in blue) and the position of inequivalent Cs sites in Cs_2CuCl_4, as denoted. The color (shades of gray) coding for Cs sites refers to the corresponding orientation of the principal axes tensor in (a) and (b).

Table 2. The shift components in %, obtained by fitting the data to equation (12) for Cs(A) and Cs(B) at three different temperatures. Angle values are estimated with uncertainties of the order of a few tenths of a degree.

T (K)	K_a	K_b	K_c	K_{ac}	δ_K (deg)
			Cs(A)		
293	0.22	0.21	0.29	±0.04	24.4
81	0.95	0.87	1.26	±0.15	22.0
4.2	9.1	8.2	11.6	±1.75	27.2
			Cs(B)		
293	0.023	−0.014	−0.024	±0.006	−7.1
81	0.20	0.042	0.014	±0.018	−5.6
4.2	2.1	0.627	0.473	−0.55/+0.25	−13

weakly anisotropic, i.e. the tensor possesses unequal diagonal terms, with the largest shift component along the c-axis, i.e. $K_c > K_a \gtrsim K_b$. For the Cs(B) site the anisotropy is more pronounced with the largest shift component along the a-axis, $K_a \gg K_c > K_b$, in agreement with our findings in [5]. Non-zero off-diagonal shift tensor elements imply that the crystallographic axes are not the principal axes of the shift tensor. It is found that the principal axes of the shift tensor, represented in the coordinate system O_{xyz}, are rotated about the b-axis so that the z-axis makes an angle δ_K with the a-axis as depicted in figure 6. The values of the angles are $\delta_K = \pm 27°$ for Cs(A) and $\delta_K = \pm 10°$ for Cs(B).

The $H_{\rm loc}$, as defined in equation (6), that is directly related to the shift depends on the electron–nuclear interaction tensor and the Cu spin configuration. To be able to study the temperature and the field dependence of the spin configuration it is useful to separate the interaction term itself from the shift data. For ^{133}Cs NMR in Cs_2CuCl_4 the interaction tensor can be expressed as $(\mathbb{D}_N + \mathbb{A}_N)$, where $\mathbb{D}_N$ is the dipolar interaction tensor and $\mathbb{A}_N$, the transferred hyperfine tensor. Unlike the dipolar interaction term, the hyperfine tensor is difficult to calculate from first principles. Therefore, we proceed with the calculation of the dipolar tensor and will address the determination of $\mathbb{A}_N$ in the subsequent section.

3.3. Dipolar interaction

In the paramagnetic state for $H_0 = 0$ T, the net average spin is zero ($\langle \mathbf{S}_N \rangle = 0$) due to a random spin orientation. In an applied magnetic field the average value of the spin projected along the field is non-zero and independent of the position N relative to the nuclear spin: $\mathbf{S}_N = \langle S_\parallel \rangle$. Therefore, the expression for the local field at the nuclear site created by the electronic spin due to dipolar interaction can be written as:

$$\mathbf{H}_{\rm loc} = \mathbf{g}\mu_{\rm B} \sum_N \mathbb{D}_N \cdot \mathbf{S}_N \equiv \mathbf{g}\mu_{\rm B}\mathbb{D} \cdot \langle S_\parallel \rangle. \tag{14}$$

We note here that the dipolar tensor $\mathbb{D}$ is independent of N. Calculation of the dipolar interaction, therefore, only requires knowledge of the position of the interacting elements, given in [15]. To ensure convergence, the dipole interaction at each Cs site is obtained by summing the 12 nearest neighbor Cu spins in all directions. The numerical results for the $\mathbb{D}$ tensor in the coordinate system of the crystal principal axes (in the units of $[\mathrm{mT}/\mu_{\rm B}]$) are

$$\mathbb{D}^{\rm Cs(A)} = \begin{pmatrix} -3.40 & -0.01 & \pm 4.26 \\ -0.01 & +8.12 & -0.03 \\ \pm 4.26 & -0.03 & -4.72 \end{pmatrix},$$
$$\mathbb{D}^{\rm Cs(B)} = \begin{pmatrix} +13.82 & -0.04 & \pm 12.26 \\ -0.04 & -7.61 & -0.04 \\ \pm 12.26 & -0.04 & -6.21 \end{pmatrix}. \tag{15}$$

We note that for both Cs(A) and Cs(B) sites values of D_{ab}, D_{ba}, D_{bc}, and D_{cb} are negligible compared to the other components of the tensor and can be considered to be nearly zero. Therefore, the dipolar tensor has the same symmetry as the shift tensor. The off-diagonal terms, D_{ac} and D_{ca}, alternate signs for Cs atoms situated on odd and even chains. The difference between diagonal terms for even and odd chains within the unit cell is of the order of a few per cent. Above, we report their average values.

The principal axes of the $\mathbb{D}$ tensor, found by diagonalization, are rotated by an angle δ_D about the b-axis of the crystal, similar to the shift tensor, as depicted in figure 6. For the Cs(A) site the angle $\delta_D = \pm 40.7°$ for the positive and negative off-diagonal terms, respectively, while for the Cs(B) site $\delta_D = \pm 26.3°$.

Table 3. Dipolar shift in % at $T = 4.2$ K and $H_0 = 5$ T calculated using equation (16).

Cs(A)	$K_a^{\rm dip}$	$K_b^{\rm dip}$	$K_c^{\rm dip}$	$K_{ac}^{\rm dip}$
$\delta_D = \pm 49.1^\circ$	-0.031	0.069	-0.044	± 0.039
Cs(B)	$K_a^{\rm dip}$	$K_b^{\rm dip}$	$K_c^{\rm dip}$	$K_{ac}^{\rm dip}$
$\delta_D = \pm 26.3^\circ$	0.125	-0.064	-0.059	± 0.113

To calculate the shift associated with the dipolar interaction, the value of the effective spin $\langle S\rangle$ must be known. In the paramagnetic phase, the effective spin is lower than 0.5/Cu due to a random orientation of spins. Its value increases, as the applied field increases and as temperature decreases, following the Curie–Weiss law. At $T = 4.2$ K and $H_0 = 5$ T, the value of $\langle S_i\rangle \sim 0.2\mu_{\rm B}$/Cu is estimated from field dependence measurements of the shift up to the fully polarized state ($H_0 > 10$ T). The shift due to the dipolar interaction is defined as

$$K^{\rm dip} = \left(\hat{\mathbf{h}}\cdot\mathbb{D}\cdot\hat{\mathbf{h}}\right)\langle S\rangle/H_0. \tag{16}$$

Using the above equation we calculate the $K^{\rm dip}$ as a function of the magnetic field orientation at $T = 4.2$ K and $H_0 = 5$ T. The detailed results for both Cs(A) and Cs(B) sites are summarized in table 3.

The contribution of the dipolar interaction to the total shift at the Cs(A) site is negligible. Specifically, along the principal crystal axes the ratio of the dipolar contribution to the total shift equals $K_a^{\rm dip}/K_a = -0.34\%$, $K_c^{\rm dip}/K_c = -0.38\%$, $K_b^{\rm dip}/K_b = 0.84\%$ and $K_{ac}^{\rm dip}/K_{ac} = \pm 2.23\%$. At the Cs(B) site the dipolar interaction contributions to the total shift along any crystal axis are relatively weak, i.e. $K_a^{\rm dip}/K_a = 5.95\%$, $K_b^{\rm dip}/K_b = -10.2\%$, $K_c^{\rm dip}/K_c = -12.5\%$ and $K_{ac}^{\rm dip}/K_{ac} = \pm 28.3\%$.

3.4. Transferred hyperfine interaction

Evidently the dipolar interaction cannot account for the total shift. Thus, the transferred hyperfine interaction must dominate the NMR shift especially at the Cs(A) site [6]. It is extremely difficult to calculate the hyperfine interaction between a single Cu electronic spin and the Cs nucleus, since such a calculation requires precise knowledge of the electronic wavefunction. As the unpaired Cu spin spends most of its time, nearly 70%, in the 3d orbital and 12% in the 4p orbital, the Cu wavefunction shows little 's' character. Moreover, since the Cs and Cu atoms are not nearest neighbors, a direct hyperfine interaction between Cu spin and Cs nucleus is expected to be weak. Therefore, it is most likely that the hyperfine interaction is enhanced via the Cu–Cl–Cs path [6]. Even though the individual contributions are unknown, we can generally write an effective transferred hyperfine interaction for spins in the paramagnetic state as

$$\mathbf{H}_{\rm loc} = \mathbf{g}\mu_{\rm B}\sum_N \mathbb{A}_N\cdot\mathbf{S}_N \equiv \mathbf{g}\mu_{\rm B}\mathbb{A}\cdot\langle\mathbf{S}_\parallel\rangle. \tag{17}$$

In principle, $\mathbb{A}$ can be deduced from the experiment. Supposing that it is both temperature and magnetic field independent, the value of $\mathbb{A}$ can be determined by measuring the total shift along the principal crystal axes in the fully polarized state. It is assumed that $\langle S\rangle = 0.5$/Cu in the polarized state. In this case, the local internal magnetic field ($H_{\rm loc}$) at the Cs site along any of the principal crystal axes, denoted by subscript i, is given by

$$(H_{\rm loc})_i = \tfrac{1}{2}g_i\mu_{\rm B}\,(D_{ii} + A_{ii})\,. \tag{18}$$

At $T = 60$ mK in the fully polarized state, i.e. $H_0 > 10$ T, it was found that $\mathbf{H}_{\rm loc} = (1.126, 1.154, 1.451$ T) for Cs(A) and $\mathbf{H}_{\rm loc} = (0.276, 0.094, 0.087$ T) for Cs(B) [5]. Consequently, we find that the transferred hyperfine tensor is given by

$$\mathbb{A}^{\rm Cs(A)} = \begin{pmatrix} 1.00 & 0 & \pm 0.185 \\ 0 & 0.960 & 0 \\ \pm 0.185 & 0 & 1.23 \end{pmatrix},$$
$$\mathbb{A}^{\rm Cs(B)} = \begin{pmatrix} 0.226 & 0 & \pm 0.045 \\ 0 & 0.0774 & 0 \\ \pm 0.045 & 0 & 0.0526 \end{pmatrix}, \tag{19}$$

in units of [T/$\mu_{\rm B}$]. Evidently, the transferred hyperfine tensors have the same symmetry as the shift and dipolar tensors. The principal axes of the $\mathbb{A}$ tensor are rotated by an angle δ_A about the b-axis of the crystal, as depicted in figure 6. For the Cs(A) site the angle is $\delta_A = \pm 29^\circ$, while it equals $\delta_A = \pm 13^\circ$ for Cs(B) site.

The value of these angles together with the local symmetry suggest that the form of the transferred hyperfine tensor for Cs nuclei is closely related to the orientation of the surrounding Cl tetrahedra as we discuss below. Furthermore, these considerations provide a simple physical explanation of the alternating sign of the off-diagonal terms in equation (19). We consider the hyperfine interaction between the Cs and one Cu and assume that the strength of the interaction is maximum when the Cu spin is aligned with the axis of symmetry of the tetrahedra, see figure 1(a). Furthermore, we assume that in the coordinate system O_{xyz} defined by the axis of symmetry of the tetrahedra, the hyperfine tensor will be diagonal: $\mathsf{a} = \mathrm{diag}(\mathsf{a}_x, \mathsf{a}_y, \mathsf{a}_z)$. Therefore, in the coordinate system of the crystal O_{abc}, related to the O_{xyz} through a rotation of $\pm\alpha \sim 35^\circ$ away from the a-axis in the (ac)-plane [9], the hyperfine tensor takes the non-diagonal form

$$\mathsf{a}_\pm = \begin{pmatrix} \mathsf{a}_x\cos^2\alpha + \mathsf{a}_z\sin^2\alpha & 0 & \pm(\mathsf{a}_x - \mathsf{a}_z)\cos\alpha\sin\alpha \\ 0 & \mathsf{a}_y & 0 \\ \pm(\mathsf{a}_x - \mathsf{a}_z)\cos\alpha\sin\alpha & 0 & \mathsf{a}_z\cos^2\alpha + \mathsf{a}_x\sin^2\alpha \end{pmatrix}. \tag{20}$$

Here the off-diagonal terms change sign depending on the *up/down* (positive/negative angle α) orientation of the tetrahedra with respect to the (bc)-plane. The immediate electronic environment of Cs(A) consists of three tetrahedra forming a triangle with the Cs located in its center, see figure 7. On even chains, there are two *down* and one *up* such tetrahedra, while on odd chains, the configuration is two *up* and one *down*. Supposing that only these three hyperfine interactions $\mathsf{a}_\pm$ equally contribute to the net hyperfine interaction, one obtains

$$\mathbb{A}^{\rm Cs(A_1)} \simeq 2\mathsf{a}_- + \mathsf{a}_+ \qquad \text{and} \qquad \mathbb{A}^{\rm Cs(A_2)} \simeq 2\mathsf{a}_+ + \mathsf{a}_-. \tag{21}$$

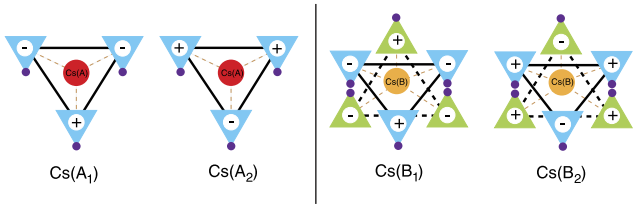

Figure 7. Scheme of the transferred hyperfine interaction for $Cs(A_1)$, $Cs(A_2)$, $Cs(B_1)$, and $Cs(B_2)$. The orientation of the Cl tetrahedra is depicted by triangles. The $+/-$ signs refer to *up/down* orientation of the axis of symmetry of the tetrahedra with respect to the (bc)-plane. The dots indicate the direction of the axis of symmetry of the tetrahedra, denoted by arrows and dashed lines in figure 1(a).

The off-diagonal terms of the net tensor change sign, thus, creating two inequivalent Cs sites. Moreover, the principal axes of this net tensor differ from the ones of the tetrahedra most likely by an angle close to α ($\delta_k \approx \alpha$). This is because the three tetrahedra are situated at approximately equal distances from the cesium atom. In the case of the Cs(B), the atom is situated nearly in the middle of two planes with opposite tetrahedra configuration as illustrated in figure 7. As a consequence, the net hyperfine interaction could be strongly attenuated on the Cs(B) site, since the contribution of one plane cancels the contribution from the other one. However, the anisotropic electronic environment of the Cs(B) results in an incomplete cancelation. This explains the smaller values of the Cs(B) hyperfine tensor elements that are $\sim$10% of those of the Cs(A), as well as the smaller angle $\delta_K = \pm 10^\circ$ found experimentally.

4. Conclusion

An extensive ^{133}Cs NMR study of the magnetic insulator Cs_2CuCl_4 in its paramagnetic phase as a function of the orientation of an applied magnetic field with respect to the principal crystalline axes is presented. The full transferred hyperfine tensor for the two inequivalent Cs sites of the unit cell was deduced. The tensors are anisotropic and their principal axes do not coincide with those of the crystal. The transferred hyperfine coupling between Cu electronic spins and Cs nuclei dominates the NMR shift on one of the Cs sites.

Acknowledgments

The work was supported in part by the National Science Foundation (DMR-0547938). A portion of this work was performed at the National High Magnetic Field Laboratory, which is supported by NSF Cooperative Agreement No. DMR-0084173, by the State of Florida, and by the DOE.

References

[1] Coldea R *et al* 2001 *Phys. Rev. Lett.* **86** 1335
[2] Coldea R *et al* 2003 *Phys. Rev.* B **68** 134424
[3] Tokiwa Y *et al* 2006 *Phys. Rev.* B **73** 134414
[4] Veillette M Y and Chalker J T 2006 *Phys. Rev.* B **74** 052402
[5] Vachon M-A *et al* 2006 *New J. Phys.* **8** 222
[6] Hartmann H, Strehlow W and Haas H 1968 *Z. Naturf.* A **23** 2029
[7] Soboleva L V *et al* 1981 *Krystallografiya* **26** 817
[8] Bailleul S *et al* 1991 *C.R. Acad. Sci.* 2 **313** 1149
[9] Bailleul S *et al* 1994 *Eur. J. Solid State Inorg. Chem.* **31** 431
[10] Coldea R *et al* 1996 *J. Phys.: Condens. Matter* **8** 7473
[11] Slichter C P 1990 *Principles of Magnetic Resonance* (Berlin: Springer)
[12] Abragam A 1961 *The Principles of Nuclear Magnetism* (Oxford: Oxford University Press)
[13] Mehring M 1976 *High Resolution NMR Sprectroscopy in Solids* (*NMR Basic Principles and Progress* vol 11) (Berlin: Springer)
[14] Volkoff G M *et al* 1952 *Can. J. Phys.* **30** 270
[15] McGinnety J A 1972 *J. Am. Chem. Soc.* **94** 8406